



# Initial spread of $^{137}\text{Cs}$ from the Fukushima Dai-ichi Nuclear Power Plant over the Japan continental shelf: a study using a high-resolution, global-coastal nested ocean model

Z. Lai<sup>1,2,8</sup>, C. Chen<sup>2,7</sup>, R. Beardsley<sup>3</sup>, H. Lin<sup>2,7</sup>, R. Ji<sup>4,7</sup>, J. Sasaki<sup>5</sup>, and J. Lin<sup>6</sup>

<sup>1</sup>School of Marine Sciences, Sun Yat-Sen University, Guangzhou, 510275, China

<sup>2</sup>School for Marine Science and Technology, University of Massachusetts-Dartmouth, New Bedford, MA 02744, USA

<sup>3</sup>Department of Physical Oceanography, Woods Hole Oceanographic Institution, Woods Hole, MA 02543, USA

<sup>4</sup>Department of Biology, Woods Hole Oceanographic Institution, Woods Hole, MA 02543, USA

<sup>5</sup>Department of Socio-Cultural Environmental Studies, Graduate School of Frontier Sciences, The University of Tokyo, Kashiwanoha, Kashiwa 277-8563, Japan

<sup>6</sup>Department of Geology & Geophysics, Woods Hole Oceanographic Institution, Woods Hole, MA 02543, USA

<sup>7</sup>International Center for Marine Studies, Shanghai Ocean University, Shanghai, 201306, China

<sup>8</sup>Key Laboratory of Marine Resources and Coastal Engineering in Guangdong Province, Guangzhou, 510275, China

Correspondence to: Z. Lai (laizhig@mail.sysu.edu.cn)

Received: 31 December 2012 – Published in Biogeosciences Discuss.: 4 February 2013

Revised: 2 July 2013 – Accepted: 10 July 2013 – Published: 14 August 2013

**Abstract.** The 11 March 2011 tsunami triggered by the M9 and M7.9 earthquakes off the Tōhoku coast destroyed facilities at the Fukushima Dai-ichi Nuclear Power Plant (FNPP) leading to a significant long-term flow of the radionuclide  $^{137}\text{Cs}$  into coastal waters. A high-resolution, global-coastal nested ocean model was first constructed to simulate the 11 March tsunami and coastal inundation. Based on the model's success in reproducing the observed tsunami and coastal inundation, model experiments were then conducted with differing grid resolution to assess the initial spread of  $^{137}\text{Cs}$  over the eastern shelf of Japan. The  $^{137}\text{Cs}$  was tracked as a conservative tracer (without radioactive decay) in the three-dimensional model flow field over the period of 26 March–31 August 2011. The results clearly show that for the same  $^{137}\text{Cs}$  discharge, the model-predicted spreading of  $^{137}\text{Cs}$  was sensitive not only to model resolution but also the FNPP seawall structure. A coarse-resolution ( $\sim 2$  km) model simulation led to an overestimation of lateral diffusion and thus faster dispersion of  $^{137}\text{Cs}$  from the coast to the deep ocean, while advective processes played a more significant role when the model resolution at and around the FNPP was refined to  $\sim 5$  m. By resolving the pathways from the leaking source to the southern and northern discharge canals, the

high-resolution model better predicted the  $^{137}\text{Cs}$  spreading in the inner shelf where in situ measurements were made at 30 km off the coast. The overestimation of  $^{137}\text{Cs}$  concentration near the coast is thought to be due to the omission of sedimentation and biogeochemical processes as well as uncertainties in the amount of  $^{137}\text{Cs}$  leaking from the source in the model. As a result, a biogeochemical module should be included in the model for more realistic simulations of the fate and spreading of  $^{137}\text{Cs}$  in the ocean.

## 1 Introduction

The 11 March 2011 Tōhoku magnitude 9.0 and 7.9 earthquakes caused a massive tsunami with  $\sim 16$  m wave height nearshore and tsunami-induced inundation that devastated the eastern coast of Japan (Fig. 1). Unlike previous earthquake-induced tsunami events, the Fukushima Dai-ichi Nuclear Power Plant (FNPP) was seriously damaged, resulting in the leaking of large amounts of artificial radionuclides, mainly  $^{131}\text{I}$  ( $t_{1/2} = 8.02$  days),  $^{134}\text{Cs}$  ( $t_{1/2} = 2.065$  yr) and  $^{137}\text{Cs}$  ( $t_{1/2} = 30.17$  yr), from several reactor units into the coastal ocean (Ohnishi, 2012). In this event, the planned

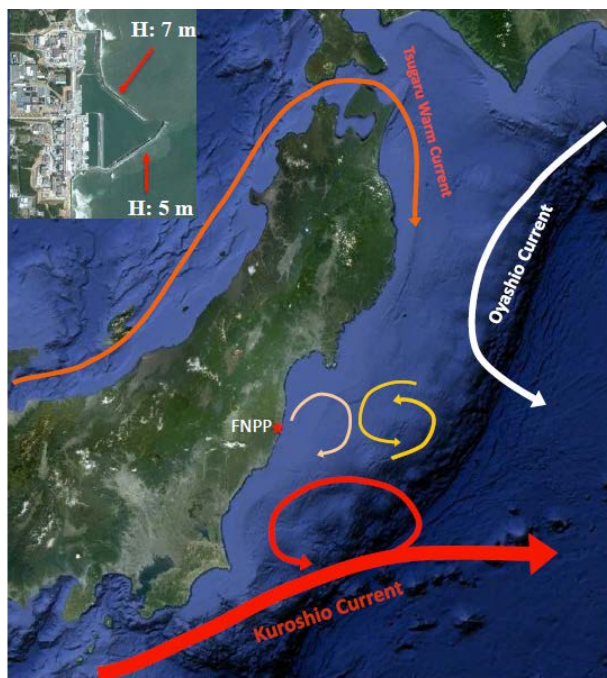


**Fig. 1.** Schematic of the regional circulation pattern with an enlarged view of the Fukushima Dai-ichi Nuclear Power Plant.

dumping from the storage room contained low-level radioactive water, while the leaking from reactors contained high-level radioactive water, with a concentration of  $9.4 \times 10^{14}$  Bq for  $^{137}\text{Cs}$  and  $^{134}\text{Cs}$  as well as  $2.8 \times 10^{15}$  Bq for  $^{131}\text{I}$  from Unit-2 over the period of 1–6 April and of  $9.8 \times 10^{12}$  Bq for  $^{137}\text{Cs}$ ,  $9.3 \times 10^{12}$  Bq for  $^{134}\text{Cs}$ , and  $9.5 \times 10^{12}$  Bq for  $^{131}\text{I}$  from Unit-3 over the period of 10–11 May. In contrast to the Chernobyl disaster in 1986, this was not the most serious radionuclide-leakage in the past. The difference is that the Chernobyl Nuclear Power Plant was located inland and its impact on the Black and Baltic Seas was through atmospheric deposition with a value of  $10^5$  Bq, much smaller than what happened at the FNPP. As a result, following the 11 March 2011 tsunami event and in addition to the wet and dry deposition from the atmosphere, the coastal water was contaminated by discharges of a large portion of high-level radioactive water out of the FNPP from leaking sources (Honda et al., 2012) and from inland-polluted rivers (Oura and Ebihara, 2012).

Among these radioactive isotopes,  $^{137}\text{Cs}$  was of particular interest because of its long 30.2 yr half-life. The accumulation of  $^{137}\text{Cs}$  in marine food chains could exert a profound impact on marine biota and human health and thus the local to regional ecosystem (Buesseler et al. 2011; Grossman, 2011). Accurately determining the initial dispersion of  $^{137}\text{Cs}$  off Japan's coast was a prerequisite for assessing its long-term impacts in the interior of the Pacific Ocean. After the leaking occurred, many efforts have been made to monitor the spread of  $^{137}\text{Cs}$  off Japan's coast. The Min-

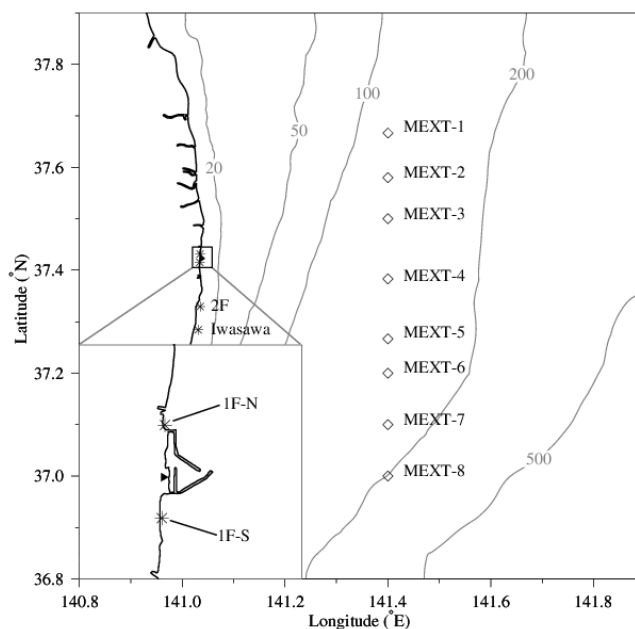


**Fig. 2.** Locations of the north discharge canal (1F-N) and the south discharge canal (1F-S), the 2F and Iwasawa stations at south of 1F-S and the eight MEXT sampling sites 30 km off the coast. The filled triangle indicates the location of the discharge source for leaking  $^{137}\text{Cs}$ .

istry of Education, Culture, Sport, Sciences and Technology (MEXT) (<http://radioactivity.nsr.go.jp/ja/list/238/list-1.html>) and the Tokyo Electric Power Company (TEPCO) (<http://radioactivity.nsr.go.jp/ja/list/239/list-1.html>) started measuring the  $^{137}\text{Cs}$  concentration around the FNPP and in the offshore coastal waters (Figs. 2 and 3). In addition to these two government-established monitoring programs, several field surveys were carried out in an offshore region to assess the spreading of  $^{137}\text{Cs}$  by oceanic currents, lateral diffusion and vertical mixing (e.g. Honda et al., 2012; Behrens et al., 2012; Dietze and Kriest, 2012). The research team led by K. Buesseler (Woods Hole Oceanographic Institution) made a comprehensive survey in the shelf and deeper waters off FNPP in June 2011 (Buesseler et al., 2012). Their survey measured  $^{137}\text{Cs}$  concentration over the inner-shelf area 30 km away from the coast and then along several transects across the Kuroshio pathway in the deep ocean (Fig. 3). The data collected from these monitoring and field surveys have provided a direct assessment of temporal change and spatial distribution of  $^{137}\text{Cs}$  concentration in the coastal waters. Due to the complex nature of advection and mixing in this coastal region, however, these data cannot alone be used to predict the spreading processes of  $^{137}\text{Cs}$  from FNPP in the shelf waters after the leaking started. This is one of the key reasons why an ocean model was proposed for this purpose.

It is not a trivial task for a model to simulate and predict accurately the spatial distribution and temporal change of the

$^{137}\text{Cs}$  concentration off the Japan coast. Since advection and mixing are two key physical processes that control the spread of  $^{137}\text{Cs}$  in ocean waters, we need an ocean model that is capable of resolving an integrated coastal and regional circulation system over scales from a few meters (small scale, e.g. around FNPP) to a few kilometers (mesoscale) over the shelf. The flow around FNPP and near the coast is mainly controlled by tidal exchange, winds and local coastal geometry and bathymetry. The circulation in this shelf region includes the Kuroshio Current on the south, the Oyashio Current on the north, the Tsugaru Current from Tsugaru Strait, and multiple eddies formed in the intersection area of these currents (Fig. 1). To simulate the outflow from FNPP, we need a model with accurate fitting of complex coastal geometry within and around FNPP. The water over the shelf was always stratified so that water temperature and salinity must be included in the model simulation. Several regional-scale ocean model exercises have been made to simulate the  $^{137}\text{Cs}$  spread from FNPP, e.g. Kawamura et al. (2011) and Tsumune et al. (2012) with a spatial resolution of 2 km or larger, and Estournel et al. (2012) with a resolution of 0.6 km. However, the water exchange between FNPP and the surrounding ocean is through a  $\sim 200$  m-narrow entrance between the two breakwaters. The distance between the two discharge canals (namely, the north and south discharge canals) is 1300 m. Without sufficient model resolution to accurately capture the complex pathways of  $^{137}\text{Cs}$  from FNPP, assessments made by these regional-scale models could be biased with large uncertainty. It is not clear, however, to what degree this bias could be. Could the bias caused by model resolution and geometric fitting issues led to a significant different conclusion about the dispersion of  $^{137}\text{Cs}$  off the Japan coast or reproduce the same distribution with just a small difference in accuracy? To our knowledge, this issue has not been well addressed yet in previous modeling experiments.

Geometric fitting of complex coastlines around FNPP and in coastal regions is a critical factor to resolve multi-scale geometrically controlled nearshore advection while sufficient model resolution is prerequisite of capturing a realistic lateral dispersion. Chen et al. (2008) conducted a model-dye comparison experiment over Georges Bank, with an aim of examining the impact of model resolution on lateral dispersion in the coastal ocean. They found that in order to simulate accurately the observed lateral dispersion within a tidal mixing front with a spatial variation scale of a few kilometers, model resolution down to  $\sim 500$  m or less was required. The overestimation of lateral dispersion due to model resolution varied in space and time, which could be 4–10 times larger as the model grid size is greater than 2–4 km. As a result, the model could point to an unrealistic conclusion that differed significantly from the dye observations. The dynamical processes off the FNPP coast are more complicated than on Georges Bank, so that failure to adequately resolve the important spatial scales in this region might lead to a large lateral dis-

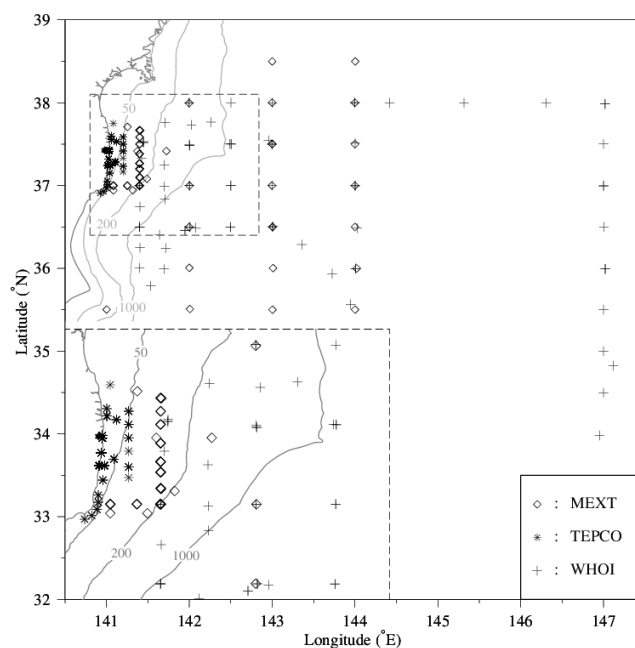


**Fig. 3.** Location of MEXT, TEPCO and WHOI monitoring and survey measurement sites. Lower-left panel is an enlarged view of the nearshore monitoring sites bounded by a dashed line box.

persion rate and thus overestimate the offshore spreading of  $^{137}\text{Cs}$  over the eastern Japan shelf.

The biggest challenge for a model to provide an accurate simulation of the spatial distribution and temporal change of  $^{137}\text{Cs}$  over the Japan shelf is the large uncertainty in the estimation of the total amount of  $^{137}\text{Cs}$  leaking into the water. The leaking lasted for months, so that the source was both spatially variable and time-dependent (Estournel et al., 2012). One approach to solve this problem is to treat  $^{137}\text{Cs}$  as a conservative tracer (without radioactive decay) and inversely determine its source amount by tracking it in the flow field for a relatively short period during which the model-predicted tracer field had the best match to observations. This method was used to evaluate the total amount of  $^{137}\text{Cs}$  from FNPP in the previous modeling experiments made by Kawamura et al. (2011), Tsumune et al. (2012), and Estournel et al. (2012). This method is generally sound, but an adjustment in this type of inverse tracking could vary from model to model, particularly for the case with different model resolutions and setups. Due to this uncertainty, the more interesting model problem, in our opinion, is on gaining knowledge of the sensitivity of the model assessment results to model skill and configuration rather than on evaluating how well a model simulates the observed  $^{137}\text{Cs}$  concentration.

We, an international research team with members from the University of Massachusetts-Dartmouth, Woods Hole Oceanographic Institution, and Yokohama National University (a member now at the University of Tokyo), have developed a high-resolution global-regional-coastal integrated

seismic-ocean-tracer FVCOM model system to simulate the March 11 earthquake-induced tsunami, coastal inundation and initial spread of  $^{137}\text{Cs}$ . Taking advantage of the geometric flexibility of the unstructured triangular grid, the model has a local resolution of up to 5 m around FNPP and near the coast. Nesting with the global-FVCOM hindcast field with data assimilation of satellite-derived sea surface temperature and sea surface height, the high-resolution regional-coastal FVCOM model not only resolved a realistic regional circulation but also provided a better representation of the water exchange between FNPP and the surrounding ocean. Built on our success in simulating the observed tsunami and coastal inundation (Chen et al., 2013), we applied this model system to track  $^{137}\text{Cs}$  over the period of 26 March–31 August 2011. Our studies aimed at assessing the impact of multi-scale physical processes on the initial spread of  $^{137}\text{Cs}$  in the coastal region of Japan, which form the foundation for more realistic simulations with the inclusion of biogeochemical processes.

## 2 The model and design of numerical experiments

The  $^{137}\text{Cs}$  was tracked as a conservative tracer in the three-dimensional (3-D) flow field predicted by the high-resolution nested global-coastal FVCOM model over the period of 26 March–31 August 2011 (Fig. 4). Hereafter we refer to the global FVCOM model as Global-FVCOM and the Japan coastal FVCOM model as JC-FVCOM. FVCOM is the prognostic, unstructured-grid Finite-Volume Community Ocean Model originally developed by Chen et al. (2003) and upgraded by the FVCOM team (Chen et al., 2006a, b, 2012). FVCOM solves the flux form of the governing equations in control volumes constructed with multi-triangular meshes using a second-order accurate discrete flux scheme, which provides accurate fitting of irregular coastal geometries and flexibility in adjusting the grid resolution to capture the key physical processes (Chen et al., 2007). The finite-volume approach ensures local mass, heat, salt, and tracer conservation in the sense of numerical computation, which is suitable to trace  $^{137}\text{Cs}$  for this study. The tracer module of FVCOM was validated through a model-dye comparison experiment made on Georges Bank in the northern North Atlantic Ocean by Chen et al. (2008).

Global-FVCOM is a fully ocean-ice coupled model covering the entire global ocean with a grid resolution of  $\sim 2$  km along the eastern Japanese coast (Fig. 4). The vertical grid discretization was implemented using a hybrid terrain-following coordinate with a total of 45 layers (Chen et al., 2013). The  $s$  coordinate was used in regions with depth greater than 225 m, in which 10 and 5 uniform layers with a thickness of 5 m were specified near the surface and bottom, respectively. The uniform thickness  $\sigma$  coordinate was employed in regions of depth less than 225 m. The coordinate transition occurred at the depth of 225 m where all layers have a uniform thickness of 5 m. Global FVCOM was

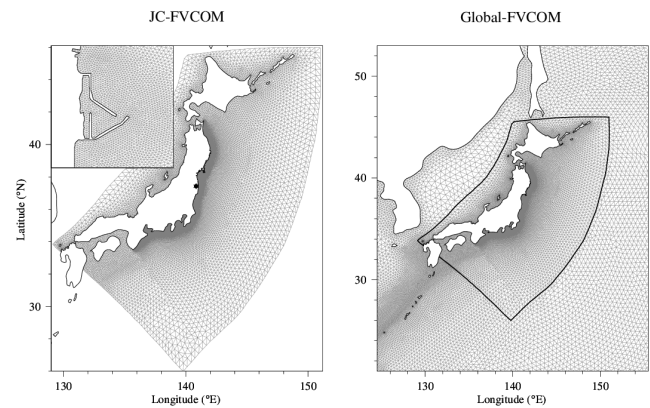


**Fig. 4.** A view of model grids for the global-Japan coastal nested FVCOM system used in this study. The Global-FVCOM grid covers the entire global ocean with a horizontal resolution of 2 km in the Japanese coastal region (shown in the right panel). The bold black line in the right panel indicates the nesting boundary that link Global-FVCOM and the Japan coastal FVCOM (JC-FVCOM). The left panel is an enlarged view of JC-FVCOM.

driven by astronomical tidal forcing with eight constituents ( $M_2$ ,  $S_2$ ,  $N_2$ ,  $K_2$ ,  $K_1$ ,  $O_1$ ,  $P_1$ , and  $Q_1$ ), the NCEP reanalysis meteorological forcing fields (surface wind stress, net heat flux/shortwave irradiation, air pressure gradients, precipitation minus evaporation ( $P - E$ )), and freshwater discharge from all major rivers along the coast. Initialized with the assimilated model fields at the end of 31 December 2010, we ran Global-FVCOM for the period of 1 January 2011–31 August 2011 for this  $^{137}\text{Cs}$  tracking experiment. To ensure that Global-FVCOM was capable of capturing the regional circulation along the eastern Japanese coast, satellite-derived sea surface temperature (SST) (<http://www.nodc.noaa.gov/SatelliteData/ghrsst>) and AVISO sea surface height (SSH) (<http://www.aviso.oceanobs.com/en/data/products/sea-surface-height-products.html>) were assimilated into the model. Global-FVCOM has been validated through a 50 yr spin-up simulation and a 33 yr (1978–2010) hindcast assimilation (Gao, 2011; Hu et al., 2011).

JC-FVCOM was configured with horizontal resolution varying from 2 km near the boundary nesting with Global-FVCOM to 5–10 m in the nearshore coastal region (including the FNPP) (Fig. 4). JC-FVCOM had the same hybrid vertical coordinate system with 45 layers and was forced with the same meteorological forcing as Global-FVCOM.

To assess the importance of resolving the detailed geometry around the leaking facility on the temporal and spatial distribution of  $^{137}\text{Cs}$  in the coastal region off Japan, we tracked  $^{137}\text{Cs}$  in two types of flow fields: One from Global-FVCOM with a horizontal resolution of 2 km along the coast around the FNPP and the other from the nested JC-FVCOM-Global-FVCOM system with a resolution of 5 m in and around the FNPP. The first set of experiments used the same approach

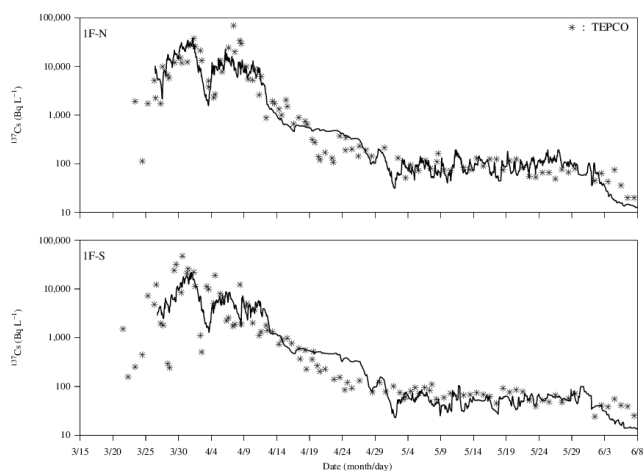


**Fig. 5.** Comparisons of model-computed and observed  $^{137}\text{Cs}$  concentrations at IF-N and IF-S over the period 26 March–8 June 2011.

as previous studies (Kawamura et al., 2011; Tsumune et al., 2012; Estournel et al., 2012), in which the  $^{137}\text{Cs}$  discharge was treated as a point source at the coast in a regional model, while the second set of experiments had sufficient resolution to simulate the  $^{137}\text{Cs}$  discharge from the FNPP through the different pathways into the ocean.

We adopted a similar approach as used by Tsumune et al. (2012) and Estournel et al. (2012) to determine inversely the amount of  $^{137}\text{Cs}$  at the source based on the best fit with observations made at the northern discharge canal (IF-N) and the southern discharge canal (IF-S) of FNPP (Fig. 2). The model-predicted  $^{137}\text{Cs}$  field was then validated with comparisons to the monitored concentrations at 2F and Iwasawa south of IF-S and other TEPCO, MEXT and WHOI measurements data made in the nearshore and offshore regions. Our estimated amount of the total direct ocean release was 14.5 PBq, which is closer to the amount of  $16.2 \pm 1.6$  PBq estimated by Rypina et al. (2013) and of 11–16 PBq estimated by Charette et al. (2013) and significantly greater than the amount of  $3.5 \pm 0.7$  PBq estimated by Tsumune et al. (2012) and 5.1–5.5 PBq estimated by Estournel et al. (2012).

In this study, direct atmospheric loading was not considered. As reported by Kawamura et al. (2011) and Tsumune et al. (2012), almost all of the  $^{137}\text{Cs}$  atmospheric deposition into the ocean occurred in March, with very little deposition afterwards. While atmospheric loading can be easily included in a tracer model, an accurate estimate of the time- and spatial-dependent  $^{137}\text{Cs}$  loading that occurred during March was not available, so previous modeling assessments were focused solely on the direct water discharge at the coast. We followed the same strategy in our tracer experiments. To avoid underestimation due to the lack of atmospheric loading, we started tracking  $^{137}\text{Cs}$  on 26 March 2011, with the understanding

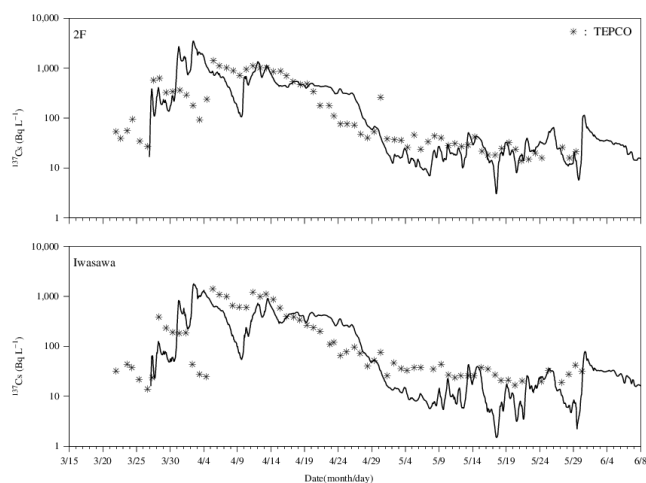


**Fig. 6.** Comparisons of model-computed and observed  $^{137}\text{Cs}$  concentrations at 2F and Iwasawa over the period 26 March–8 June 2011.

that the model-data mismatch in late March would likely be caused by atmospheric loading. Since the  $^{137}\text{Cs}$  loading from leaking sources were adjusted by best fitting with measurements at sites IF-N and IF-S at the two canal exits, the model simulation should indirectly account for some of the actual atmospheric deposition occurring in late March. Our focus here is to examine the importance of resolving the complex structure of the FNPP on predicting the initial spread of  $^{137}\text{Cs}$  in the Japanese coastal region. This approach could help us separate the impacts of the water source on the oceanic environment from the atmospheric source.

### 3 Results

#### 3.1 Comparisons with observations

The results of the high-resolution model case predicted by the nested JC-FVCOM/Global-FVCOM will be presented first, followed by a comparison with the Global-FVCOM coarse-resolution model case.

The  $^{137}\text{Cs}$  released at the nuclear reactor sites within the FNPP facility flowed out of the FNPP mainly through the channel bounded by the northern and southern breakwaters (Fig. 2; Ohnishi, 2012). In our high-resolution model case, which direction and how much  $^{137}\text{Cs}$  flowed to the IF-N and IF-S sites outside the breakwaters depended on whether or not the model was capable of resolving the local water flushing processes around FNPP. The observed  $^{137}\text{Cs}$  concentration at these two sites varied with the same trend but slightly different amplitudes, reached two peaks around the end of March and early April, and then rapidly decayed with time after 12 April 2011 (Fig. 5). By tuning the amount of  $^{137}\text{Cs}$  at the source, the high-resolution model reproduced these variations reasonably well. This suggested that the model could

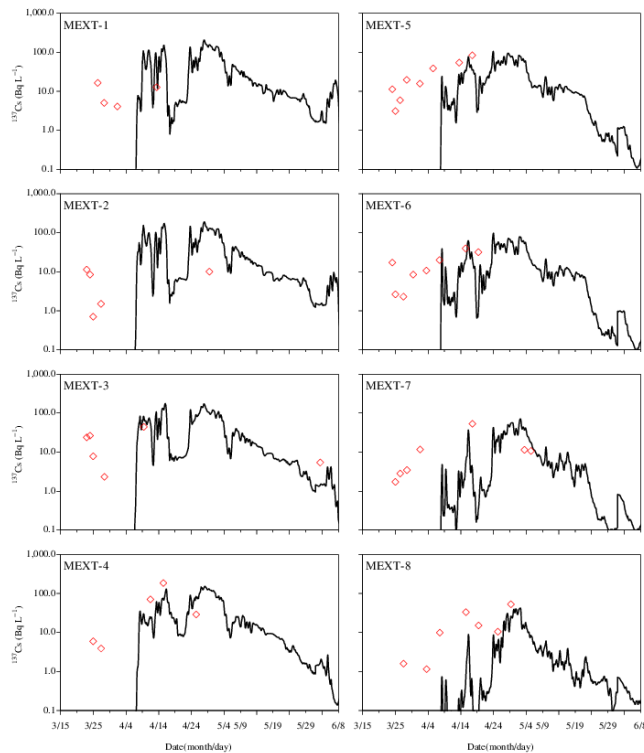


**Fig. 7.** Comparisons of model-computed and observed  $^{137}\text{Cs}$  concentrations at eight MEXT monitoring sites (30 km off the coast) for the period 1 April–8 June 2011.

provide a realistic flow exchange process between FNPP and the adjacent ocean.

Sites 2F and Iwasawa are located near the coast about 9 and 14 km south of 1F-S, respectively. The model-data comparison at these two sites again captured the observed rapid increase in  $^{137}\text{Cs}$  concentration in late March and the gradual decay trend in April (Fig. 6). However, at these sites the peak concentration of  $^{137}\text{Cs}$  was about 1–2 orders of magnitude smaller than that at 1F-S.

A further comparison was made at eight MEXT sites over the shelf (Fig. 7). The measurements suggest that, excluding atmospheric loading, a significant amount of  $^{137}\text{Cs}$  in the radioactive water from the FNPP arrived in this shelf area about two weeks after the leaking started. Although the MEXT sites were only about 30 km away from the coast, the maximum  $^{137}\text{Cs}$  concentrations were about  $10^2$ – $10^3$  lower compared with the peak values observed at the monitoring site 1F-S. The  $^{137}\text{Cs}$  concentrations at MEXT sites reached a peak value of  $\sim 100 \text{ Bq L}^{-1}$  at the end of April and then rapidly decreased to  $\sim 10 \text{ Bq L}^{-1}$  or less during May. The model-computed  $^{137}\text{Cs}$  concentration and its decay trend with time were in reasonable agreement with observations. For example, at site MEXT-3, the observed  $^{137}\text{Cs}$  concentration was slightly lower than  $100 \text{ Bq L}^{-1}$  in early April and lower than  $10 \text{ Bq L}^{-1}$  in early June. These two values

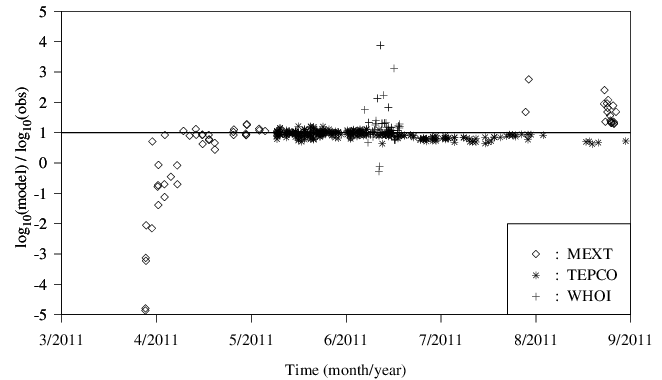


**Fig. 8.** Logarithmic ratio of the high-resolution nested model-computed surface  $^{137}\text{Cs}$  concentration to the observation at MEXT, TEPCO and WHOI measurement sites over the period 26 March–31 August 2011.

and varying trends were well captured by the model. For the same given time period, the model suggested that the  $^{137}\text{Cs}$  concentrations were higher at the northern sites than at the southern sites. It is thought that the  $^{137}\text{Cs}$  detected at the MEXT sites before 8 April was due to atmospheric deposition (Kawamura et al., 2011; Estournel et al., 2012; Tsumune et al., 2012). Since neither atmospheric deposition nor an initial field of  $^{137}\text{Cs}$  concentration was set up in the current study, no direct comparison with observational value recorded during that period should be made.

We then compared the model-computed  $^{137}\text{Cs}$  concentrations with observations at the same location and time where/when measurements were made for all available data sources, including TEPCO, MEXT, and WHOI. At the surface (Fig. 8), starting in early April, the model-computed  $^{137}\text{Cs}$  concentration showed a good match with MEXT and TEPCO measurements, even though a large uncertainty exists about the initial  $^{137}\text{Cs}$  distribution, loading from atmospheric deposition and point source as well as the complex biogeochemical processes in seawater. A mismatch appeared in late March that was likely a result of atmospheric deposition, which was omitted in our study. TEPCO measurement sites were located in the nearshore regions close to FNPP. Reasonably good agreement between model-computed and observed  $^{137}\text{Cs}$  concentrations for TEPCO data in April through August suggests that the high-resolution model succeeded in resolving the advection and dispersion processes near the coast. A good match was also found for MEXT data from April to May, indicating that the model was also robust to capture these physical processes in the inner shelf region over a time scale of a month after leaking started. The model, however, tended to overestimate the  $^{137}\text{Cs}$  concentrations recorded during the WHOI June survey and at MEXT sites in August. The WHOI survey started with one transect roughly around the 200 m isobath 30 km from the coast followed by other transects across the slope and eastward

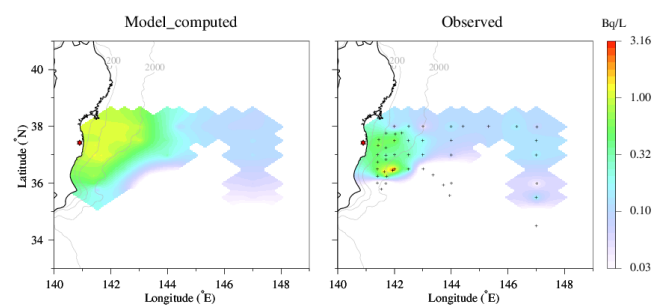


**Fig. 9.** Comparisons of high-resolution nested model-computed and observed (from the June WHOI survey) surface  $^{137}\text{Cs}$  concentrations at the survey sites in June 2011.

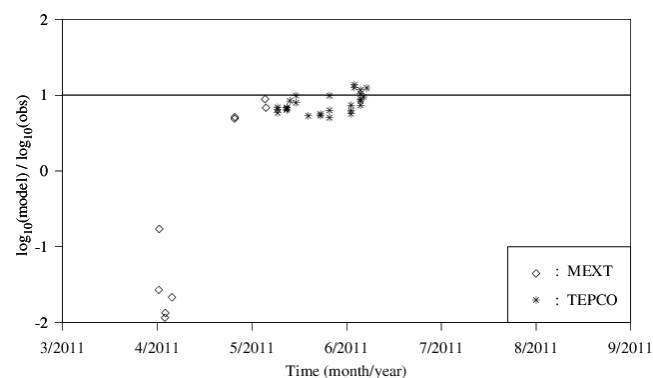


**Fig. 10.** Logarithmic ratio of the model-computed  $^{137}\text{Cs}$  bottom concentration to the observation at MEXT and TEPCO measurement sites over the period 26 March–31 August 2011.

Kuroshio main stream. Placing both model-computed and observed  $^{137}\text{Cs}$  concentrations at measurement sites and creating images based on these data (Fig. 9), we can see that the model was robust in predicting the spatial distribution of  $^{137}\text{Cs}$  concentration that were observed during the WHOI June survey, but it tended to overestimate the size of the  $^{137}\text{Cs}$  concentration plume and its values in the mid-shelf and slope regions.

Near the ocean bottom (Fig. 10), however, the model-computed  $^{137}\text{Cs}$  concentration was generally lower than the observed values at both TEPCO and MEXT monitoring sites. The overestimation at the surface and underestimation near the bottom imply that in addition to vertical diffusion and mixing, there were other physical processes that were responsible for a downward flux of  $^{137}\text{Cs}$  in the water column. By adding a sinking term in the  $^{137}\text{Cs}$  tracer model, one should be able to improve the simulation results. The critical issue is that such a sinking term is related to sedimentation over the shelf with the sinking velocity varying significantly with different types of sediments. We will discuss this issue in the next section.

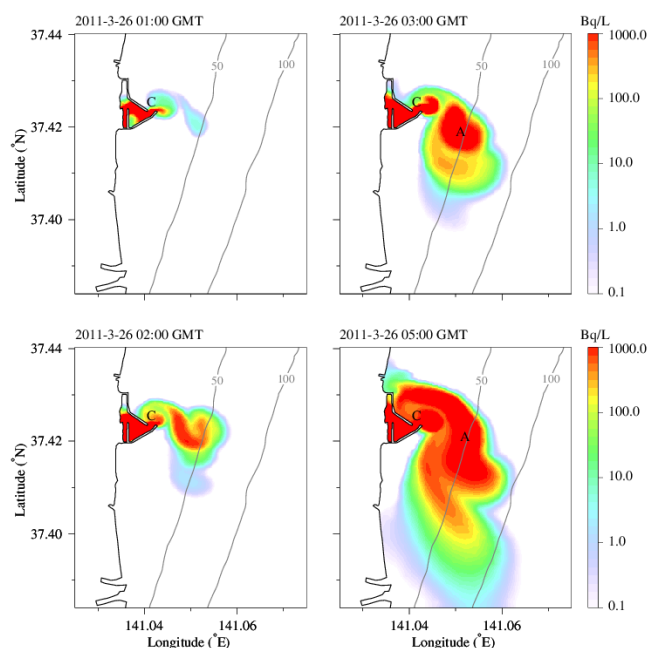


**Fig. 11.** Distributions of the high-resolution nested model computed surface  $^{137}\text{Cs}$  concentration around FNPP at 01:00, 02:00, 03:00 and 04:00 GMT, 26 March 2011. Label “C” indicates the location of a cyclonic vortex, and label “A” indicates the location of an anti-cyclonic vortex.

### 3.2 Comparisons between high- and coarse-resolution models

Most of the  $^{137}\text{Cs}$  was transported into the Japan’s coastal shelf through a pumping-like process from the narrow exit between the northern and southern breakwaters of FNPP. As a result of tidal flushing and dumping of cooling water into FNPP, the maximum outflow at the exit was about  $2\text{ m s}^{-1}$ . This strong outflow was jet-like and formed a cyclonic vortex initially due to shear instability (Fig. 11). With a continuous supply of water from the exit, this vortex became large and then separated into several large cyclonic and anticyclonic vortices in late March before entering the continental shelf where the regional-scale circulation became dominant. Once the  $^{137}\text{Cs}$  tracer was over the shelf where the water depth was 50–100 m or deeper, its spread was strongly influenced by the local wind and regional circulation (Fig. 12). In April, the tracer appeared like a coastal plume, which moved back and forth in the south–north direction along the coast. In May, the  $^{137}\text{Cs}$  plume was still constrained within the coastal region but had a significant southward transport. It arrived in the southern region about 180 km south of FNPP in mid-May, where a portion of the  $^{137}\text{Cs}$  was carried offshore by the eastward-flowing Kuroshio Current. At the same time, the northward wind caused coastal upwelling and wind-induced Ekman flow advected and dispersed the  $^{137}\text{Cs}$  plume offshore. In July and August, the plume was predominantly

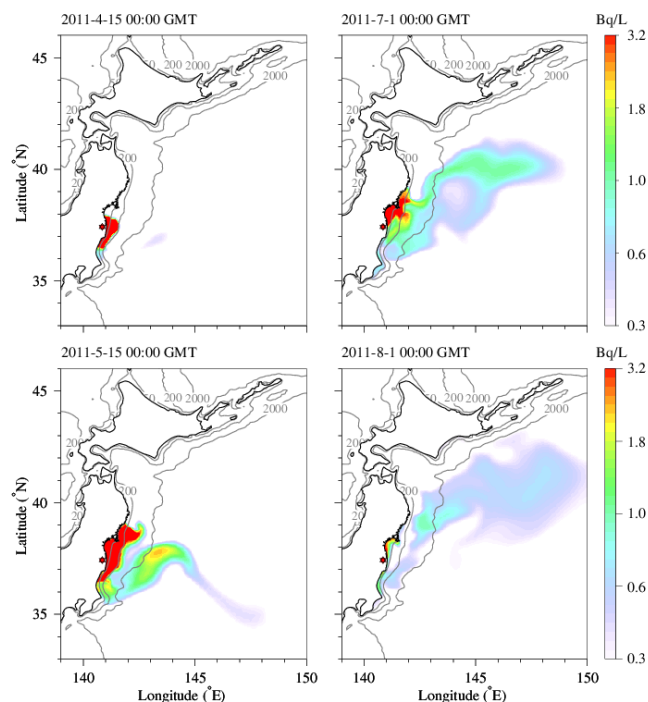


**Fig. 12.** Distributions of the high-resolution nested model computed surface  $^{137}\text{Cs}$  concentration in Japan's coastal region at 15:00 GMT 15 April; 15:00 GMT 15 May; 00:00 GMT 1 July; and 00:00 GMT 1 August 2011.

transported towards the north and gradually dispersed into the interior of the Pacific Ocean. These results are consistent with the  $^{137}\text{Cs}$  samples collected at Hasaki (a coastal station 180 km south of FNPP) by Aoyama et al. (2012) as well as measurements made at ten sites along the northern coast of Sanriku and Tsugaru Strait north of FNPP by Inoue et al. (2012).

To our knowledge, all previous model assessments of the  $^{137}\text{Cs}$  spreading were made with a regional-scale model without resolving the geometry of FNPP. Key questions here include is the initial pumping process from FNPP critical for a model to produce a realistic spread of  $^{137}\text{Cs}$  from the FNPP, or could the nearshore process be ignored if one is only interested in predicting the  $^{137}\text{Cs}$  spread over a regional scale? To address these questions, we followed the methods used in previous model assessments and tracked  $^{137}\text{Cs}$  in the flow field predicted by Global-FVCOM.

In this regional model case, because the 2 km resolution grid was unable to resolve the FNPP facility and breakwater complex, the leaking  $^{137}\text{Cs}$  was treated as a point source with the same rate of release used in the high-resolution model. The resulting spread of  $^{137}\text{Cs}$  predicted by Global-FVCOM differed significantly from the high-resolution model case. At 04:00 GMT 26 March, for example, the high-resolution nested model showed that the  $^{137}\text{Cs}$  tracer was still around the FNPP exit, but the Global-FVCOM-computed  $^{137}\text{Cs}$  con-

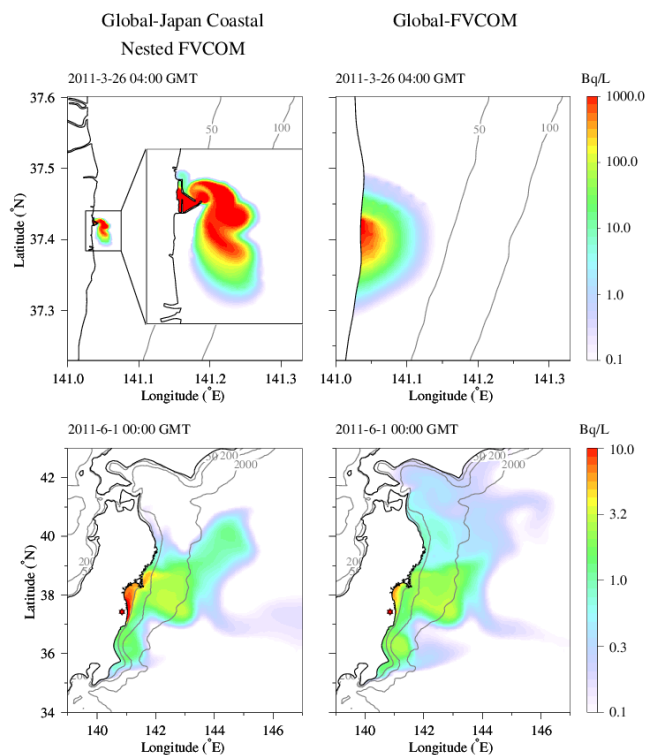


**Fig. 13.** Comparisons of distributions of the  $^{137}\text{Cs}$  concentrations predicted by the nested Global-FVCOM and JC-FVCOM model (left panels) and the Global-FVCOM (right panels) at 04:00 GMT 26 March and 00:00 GMT 1 June 2011.

centration was distributed symmetrically surrounding the point source and covered a much larger area with a width of  $\sim 0.2^\circ$  in latitude along the coast (Fig. 12: upper panels). At 00:00 GMT 1 June, the  $^{137}\text{Cs}$  concentration predicted by Global-FVCOM had spread in the entire shelf and slope region up to  $43^\circ\text{N}$ , while the  $^{137}\text{Cs}$  concentration computed by the high-resolution nested model remained high near the coast and no tracer was found north of  $41^\circ\text{N}$  (Fig. 12: lower panels). It is clear that Global-FVCOM significantly overestimated the size of the plume. As a result, the model-computed  $^{137}\text{Cs}$  concentrations were significantly lower than observations at both nearshore and offshore measurement sites (Fig. 13).

The high- and coarse-resolution model results can help us understand why previous modeling efforts failed to reproduce the temporal variation of the  $^{137}\text{Cs}$  concentration over the shelf region. Applying a 2 km-resolution Regional Ocean Model System (ROMs) to the Japanese coast, Tsumune et al. (2012) conducted a tracer experiment to predict the  $^{137}\text{Cs}$  spread over the shelf. The model did capture the  $^{137}\text{Cs}$  concentration peak at MEXT-8 in mid-April, but significantly underestimated  $^{137}\text{Cs}$  concentrations at the other MEXT-1 to MEXT-7 sites. Coincidentally, Estournel et al. (2012) reported that their model also underestimated  $^{137}\text{Cs}$  concentrations at all MEXT sites, even though they increased the grid



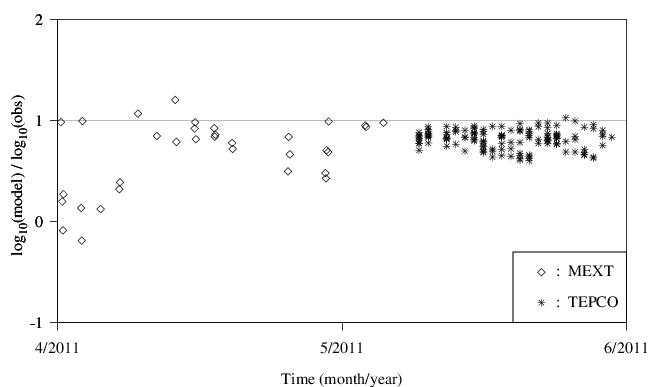


**Fig. 14.** Logarithmic ratio of the Global-FVCOM-computed surface  $^{137}\text{Cs}$  concentration to the observation at MEXT and TEPCO measurement sites during April and May 2011.

resolution to 600 m. They attributed this underestimation to the lack of information on the river discharge in the model which could cause a thin, low-salinity surface layer and enhance the offshore transport under the influence of wind. Our results, however, suggest that in order to reproduce the observed spread of  $^{137}\text{Cs}$  over the shelf, a model needs to resolve the realistic coastal geometry of the FNPP and adjacent region. In order to reproduce the dispersion process from the leaking source to 1F-N and 1F-S, a model must be capable of resolving the complex small-scale vortex current field that controlled the water exchange or pumping around FNPP. Failure to capture this initial pumping process could lead to the unrealistic  $^{137}\text{Cs}$  spreading over the shelf.

As we pointed out in the introduction, the spread of  $^{137}\text{Cs}$  is controlled mainly by advection and dispersion processes. Chen et al. (2008) analytically derived the governing equations controlling the movement of the center of a small-scale dye patch in the coastal ocean. The equations indicate that after the dye is released, the movement of the dye patch is driven by the ensemble velocity integrated through the dye patch and the concentration flux related to the vertical shear of the horizontal velocity of the dye patch. Considering a dye patch that moves conservatively in the ocean, the total amount of the dye remains unchanged, but its concentration can change significantly as a result of deformation of the dye patch due to vertical and lateral dispersion that are related to velocity shears and turbulent diffusion. In order to capture the dye spreading, it is critical to resolve the realistic vertical and lateral diffusion processes. For many coastal ocean models, the horizontal diffusion is parameterized using a Smagorinsky eddy parameterization method (Smagorinsky, 1963), which depends on the model resolution and velocity shears.

Our results indicate that an underestimation of  $^{137}\text{Cs}$  concentration over the shelf predicted by Global-FVCOM was mainly due to the overestimation of  $^{137}\text{Cs}$  spreading in the coastal region. This overestimation was caused by insuffi-

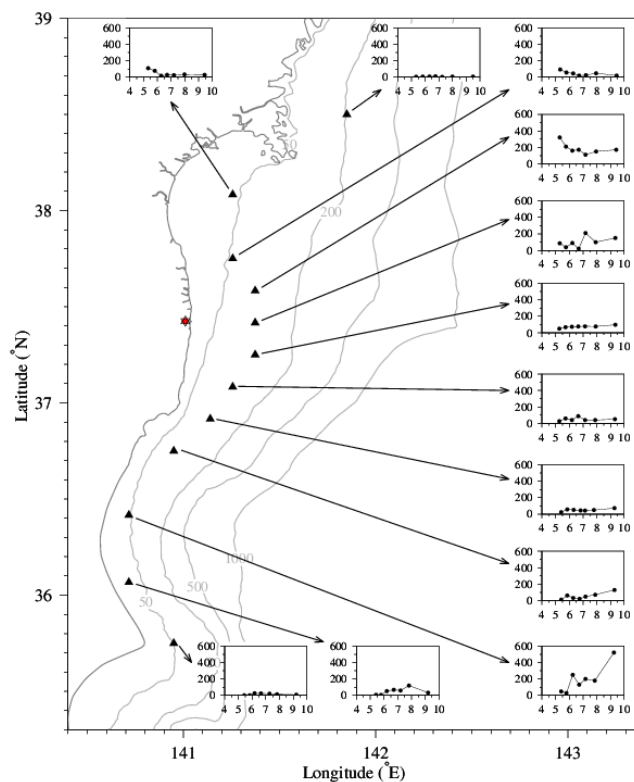


**Fig. 15.** Time series of the  $^{137}\text{Cs}$  concentration (unit:  $\text{Bq kg}^{-1}$ ) measured in sediments in the outer-shelf monitoring sites during April to October 2011.

cient grid resolution to capture realistic lateral diffusion. This explanation can be applied to previous regional model simulations and emphasize the critical importance of model resolution in the parameterization of lateral diffusion.

#### 4 Discussion

Like previous modeling efforts, we treated  $^{137}\text{Cs}$  as a dissolved conservative tracer without including biogeochemical processes through interactions with suspended matter and releases from re-suspended sediments as well as sedimentation. The overestimation at the surface and underestimation near the bottom in the model-predicted  $^{137}\text{Cs}$  concentration suggest that sedimentation processes should be included if one tries to make a more realistic prediction of the spread of  $^{137}\text{Cs}$  over the shelf. This finding was also anticipated by Estournel et al. (2012) who suggested that an overestimation of the predicted  $^{137}\text{Cs}$  concentration can probably be caused by ignoring a sinking term in the tracer equation. The suggestions from these modeling experiments are seemingly supported by the  $^{137}\text{Cs}$  concentration levels found in the bottom sediment layer at monitoring sites along the Japanese coast. At many monitoring sites in the shelf region between the 50 m and 200 m isobaths, the observed  $^{137}\text{Cs}$  concentration

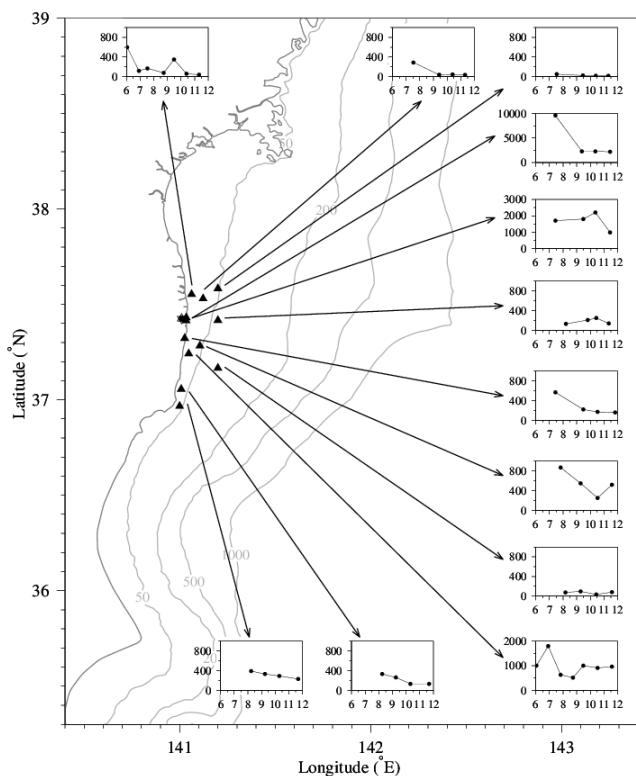


**Fig. 16.** Time series of the  $^{137}\text{Cs}$  concentration (unit:  $\text{Bq kg}^{-1}$ ) measured in sediments in the nearshore monitoring sites during June–December 2011.

in sediments increased significantly with time (Fig. 14). In monitoring sites around FNPP, the sediment  $^{137}\text{Cs}$  concentrations showed high values before July and then decreased rapidly with time afterward (Fig. 15). A simple estimation indicates that during April–June, the model-data discrepancy values at the surface and near the bottom were about 48 % and –39 % in the coastal area. Therefore, without adding a sinking term in the  $^{137}\text{Cs}$  tracer equation, about 9 % more of the total amount of  $^{137}\text{Cs}$  remained in the seawater than what was measured. Assuming these extra amounts were all deposited in the sediment through sedimentation, this means that about 9 % of the discharged  $^{137}\text{Cs}$  could be removed by sedimentation. This value is much higher than the 0.1–2 % estimated by Honda et al. (2012) in traps and Kusakabe et al. (2013) in the upper 3 cm of surface sediment at monitoring sites, implying that the 9 % unbalanced amount of  $^{137}\text{Cs}$  was not caused only by missing sedimentation. Since the uncertainty of  $^{137}\text{Cs}$  loading at 1F-S and 1F-N was at a level of 15 % relative to the total release amount, the missed sedimentation processes in the tracer model could be at the same level as that observed by Honda et al. (2012) and Kusakabe et al. (2013).

## 5 Summary

A high-resolution, global-coastal nested ocean model was developed to simulate the initial spreading of  $^{137}\text{Cs}$  over the Japan shelf after the 11 March 2011 Fukushima Dai-ichi Nuclear Power Plant failure. With sufficient resolution to resolve the complex water exchange process between the FNPP and adjacent coastal ocean, this nested model succeeded in reproducing the temporal variation and spatial distribution of  $^{137}\text{Cs}$  over the shelf during the April–August 2011 period. The comparison between high-resolution nested and regional-scale models clearly showed that given the same discharge of  $^{137}\text{Cs}$ , the model-predicted spreading of  $^{137}\text{Cs}$  was sensitive not only to model resolution but also to geometric fitting. Failure to capture this initial dispersion process from the leaking source to the 1F-N and 1F-S monitoring sites could lead to an unrealistic prediction of  $^{137}\text{Cs}$  spreading over the shelf. A coarse-resolution ( $\sim 2$  km) regional scale model overestimated lateral diffusion and thus caused faster dispersion of  $^{137}\text{Cs}$  from the coast to the deep ocean.

The  $^{137}\text{Cs}$  spreading process predicted by the high-resolution nested model was in good agreement with measurements over the inner shelf, but showed an overestimation at the surface and underestimation near the bottom in the off-shore region. These model-data discrepancies were mainly due to an uncertainty of  $^{137}\text{Cs}$  loading from sources and the assumption that treated  $^{137}\text{Cs}$  as a dissolved conservative tracer without inclusion of biogeochemical and sedimentation processes.

*Acknowledgements.* We would like to thank K. Buesseler and S. Jayne at WHOI who shared their research results and June 2011 survey data with us. We also appreciate the comments and suggestions made by K. Buesseler and M. Bacon at WHOI. This project was supported by the US National Science Foundation RAPID grants No. 1141697 and No. 1141785 and the Japan Science and Technology Agency J-RAPID program. The development of Global-FVCOM was supported by NSF grants ARC0712903, ARC0732084, and ARC0804029. Z. Lai's contribution was supported by the Natural Science Foundation of China project 41206005, China MOST project 2012CB956004, and Sun Yat-Sen University 985 grant 42000-3281301. C. Chen serves as chief scientist for the International Center for Marine Studies, Shanghai Ocean University, and his contribution was supported by the Program of Science and Technology Commission of Shanghai Municipality (09320503700).

Edited by: M. Dai

## References

- Aoyama, M., Tsumune, D., Uematsu, M., Kondo, F., and Hamajima, Y.: Temporal variation of  $^{134}\text{Cs}$  and  $^{137}\text{Cs}$  activities in surface water at stations along the coastline near the Fukushima Dai-ichi Nuclear Power Plant accident site, Japan, *Geochem. J.*, 46, 321–325, 2012.
- Behrens, E., Schwarzkopf, F. U., Lübbecke, J. F., and Böning, C. W.: Model simulations on the long-term dispersal of  $^{137}\text{Cs}$  released into the Pacific Ocean off Fukushima, *Environ. Res. Lett.*, 7, 034004, doi:10.1088/1748-9326/7/3/034004, 2012.
- Buesseler, K., Aoyama, M., and Fukasawa, M.: Impacts of the Fukushima Nuclear Power Plants on marine radioactivity, *Environ. Sci. Technol.*, 45, 9931–9935, 2011.
- Buesseler, K., Jayne, S., Fisher, N., Rypina, I., Baumann, H., Baumann, Z., Breier, C., Douglass, E., George, J., Macdonald, A., Miyamoto, H., Nishikawa, J., Pike, S., and Yoshida, S.: Fukushima-derived radionuclides in the ocean and biota off Japan, *Proc. Natl. Acad. Sci.*, 109, 5984–5988, 2012.
- Charette, M. A., Breier, C. F., Henderson, P. B., Pike, S. M., Rypina, I. I., Jayne, S. R., and Buesseler, K. O.: Radium-based estimates of cesium isotope transport and total direct ocean discharges from the Fukushima Nuclear Power Plant accident, *Biogeosciences*, 10, 2159–2167, doi:10.5194/bg-10-2159-2013, 2013.
- Chen, C., Liu, H., and Beardsley, R.: An unstructured grid, finite-volume, three dimensional, primitive equations ocean model: Application to coastal ocean and estuaries, *J. Atmos. Oc. Technol.*, 20, 159–186, 2003.
- Chen, C., Beardsley, R. C., and Cowles, G.: An unstructured grid, finite-volume coastal ocean model (FVCOM) system, Special Issue entitled “Advances in Computational Oceanography”, *Oceanography*, 19, 78–89, 2006a.
- Chen, C., Cowles, G., and Beardsley, R. C.: An unstructured grid, finite-volume coastal ocean model: FVCOM User Manual, Second Edition, SMASST/UMASSD Technical Report-06-0602, 315 pp., 2006b.
- Chen, C., Huang, H., Beardsley, R. C., Liu, H., Xu, Q., and Cowles, G.: A finite-volume numerical approach for coastal ocean circulation studies: Comparisons with finite difference models, *J. Geophys. Res.*, 112, C03018, doi:10.1029/2006JC003485, 2007.
- Chen, C., Xu, Q., Houghton, R., and Beardsley, R. C.: A model-dye comparison experiment in the tidal mixing front zone on the southern flank of Georges Bank, *J. Geophys. Res.*, 113, C02005, doi:10.1029/2007JC004106, 2008.
- Chen, C., Lai, Z., Beardsley, R. C., Sasaki, J., Lin, J., Lin, H., and Ji, R.: The 11 March 2011 Tōhoku M9.0 earthquake-induced tsunami and coastal inundation along the Japanese coast: A model assessment, *J. Geophys. Res.*, in revision, 2013.
- Dietze, H. and Kriest, I.:  $^{137}\text{Cs}$  off Fukushima Dai-ichi, Japan – model based estimates of dilution and fate, *Ocean Sci.*, 8, 319–332, doi:10.5194/os-8-319-2012, 2012.
- Estournel, C., Bosc, E., Bocquet, M., Ulses, C., Marsaleix, P., Winiarek, V., Osvath, I., Nguyen, C., Duhaut, T., Lyard, F., Michaud, H., and Auchair, F.: Assessment of the amount of cesium-137 released into the Pacific Ocean after the Fukushima accident and analysis of its dispersion in Japanese coastal waters, *J. Geophys. Res.*, 117, C11014, doi:10.1029/2012JC007933, 2012.
- Gao, G., Chen, C., Qi, J., and Beardsley, R. C.: An unstructured-grid, finite-volume sea ice model: development, validation and application. *J. Geophys. Res.*, 116, C00D04, doi:10.1029/2010JC006688, 2011.
- Grossman, E.: Radioactivity in the Ocean: Diluted, But Far from Harmless, online: [http://e360.yale.edu/feature/radioactivity\\_in\\_the\\_ocean\\_diluted\\_but\\_far\\_from\\_harmless/2391/](http://e360.yale.edu/feature/radioactivity_in_the_ocean_diluted_but_far_from_harmless/2391/), 2011.
- Honda, M. C. H., Aono, T., Aoyama, M., Hamajima Y., Kawakami, H., Kitamura M., Masumoto Y., Miyazawa Y., Takigawa M., and Saino, T.: Dispersion of artificial caesium-134 and -137 in the western North Pacific one month after the Fukushima accident, *Geochem. J.*, 46, 1–9, 2012.
- Hu, S., Chen, C., Ji, R., Townsend, D. C., Tian, R., Beardsley, R. C., and Davis, C.: Effects of surface forcing on interannual variability of the fall phytoplankton bloom in the Gulf of Maine revealed using a process-oriented model, *Mar. Ecol. Prog. Ser.*, 427, 29–49, doi:10.3354/meps09043, 2011.
- Inoue, M., Kofuji, H., Hamajima, Y., Nagao, S., Yoshida, K., and Yamamoto, M.:  $^{134}\text{Cs}$  and  $^{137}\text{Cs}$  activities in coastal seawater along Northern Sanriku and Tsugaru Strait, northeastern Japan, after Fukushima Dai-ichi Nuclear Power Plant accident, *J. Environ. Radio.*, 111, 116–119, 2012.
- Kawamura, H., Kobayashi, T., Furuno, A., In, T., Ishikawa, Y., Nakayama, T., Shima, S., and Awaji T.: Preliminary numerical experiments on oceanic dispersion of  $^{131}\text{I}$  and  $^{137}\text{Cs}$  discharged into the ocean because of the Fukushima Daiichi Nuclear Power Plant disaster, *J. Nucl. Sci. Technol.*, 48, 1349–1356, 2011.
- Kusakabe, M., Oikawa, S., Takata, H., and Misonoo, J.: Spatiotemporal distributions of Fukushima-derived radionuclides in surface sediments in the waters off Miyagi, Fukushima, and Ibaraki Prefectures, Japan, *Biogeosciences Discuss.*, 10, 4819–4850, doi:10.5194/bgd-10-4819-2013, 2013.
- Ohnishi, T.: The disaster at Japan’s Fukushima-Daiichi Nuclear Power Plant after the 11 March 2011 earthquake and tsunami, and the resulting spread of radioisotope contamination, *Radiat. Res.*, 177, 1–14, 2012.
- Oura, Y. and Ebihara, M.: Radioactivity concentrations of  $^{131}\text{I}$ ,  $^{134}\text{Cs}$  and  $^{137}\text{Cs}$  in river water in the Greater Tokyo Metropolitan area after the Fukushima Daiichi Nuclear Power Plant accident, *Geochem. J.*, 46, 303–309, 2012.
- Rypina, I. I., Jayne, S. R., Yoshida, S., Macdonald, A. M., Douglass, E., and Buesseler, K.: Short-term dispersal of Fukushima-derived radionuclides off Japan: modeling efforts and model-data intercomparison, *Biogeosciences Discuss.*, 10, 1517–1550, doi:10.5194/bgd-10-1517-2013, 2013.
- Smagorinsky, J.: General circulation experiments with the primitive equations, I. The basic experiment, *Monthly Weather Rev.*, 91, 99–164, 1963.
- Tsumune, D., Tsubono, T., Aoyama, M., and Hirose, K.: Distribution of oceanic  $^{137}\text{Cs}$  from the Fukushima Daiichi Nuclear Power Plant simulated numerically by a regional ocean model, *J. Environ. Radio.*, 111, 100–108, 2012.